Diffractive Imaging Using Partially Coherent X Rays

L. W. Whitehead, G. J. Williams, H. M. Quiney, D. J. Vine, R. A. Dilanian, S. Flewett, and K. A. Nugent
School of Physics, The University of Melbourne, Victoria 3010, Australia

A. G. Peele and E. Balaur
Department of Physics, La Trobe University, Bundoora, Victoria 3086, Australia

I. McNulty
Advanced Photon Source, Argonne National Laboratory, 9700 South Cass Avenue, Argonne, Illinois, 60439, USA
(Received 26 August 2009; revised manuscript received 18 November 2009; published 11 December 2009)

The measured spatial coherence characteristics of the illumination used in a diffractive imaging experiment are incorporated in an algorithm that reconstructs the complex transmission function of an object from experimental x-ray diffraction data using 1.4 keV x rays. Conventional coherent diffractive imaging, which assumes full spatial coherence, is a limiting case of our approach. Even in cases in which the deviation from full spatial coherence is small, we demonstrate a significant improvement in the quality of wave field reconstructions. Our formulation is applicable to x-ray and electron diffraction imaging techniques provided that the spatial coherence properties of the illumination are known or can be measured.

DOI: 10.1103/PhysRevLett.103.243902 PACS numbers: 42.30.Wb, 07.85.Qe, 42.25.Kb, 42.30.Rx

Coherent diffractive imaging (CDI) is a method by which the transmission function of a nonperiodic object is recovered from its x-ray diffraction pattern [1]. The finite extent of the scattering object establishes the uniqueness of the mapping between the wave field that exits the object and its far-zone diffraction pattern [2]. This relationship is determined iteratively, imposing whatever *a priori* information is available on the form of the complex wave field that is propagated between object and detector planes. Interest in the method has been stimulated recently by the possibility of imaging single molecules using an x-ray free-electron laser [3] and by the promising results that have been achieved using free-electron lasers in the extreme ultraviolet region [4]. While imaging of single molecules is an important goal, CDI already offers considerable promise for high-resolution imaging of three-dimensional [5] and extended [6] objects using third-generation synchrotron sources. A number of synchrotron-based applications of these methods have emerged in the biological [7] and materials sciences [8].

In most CDI work to date it has been assumed that the illuminating beam is completely coherent, an assumption that is not generally appropriate for the x-ray wave field generated by a third-generation undulator source [9,10], or even a free-electron laser source [11]. Theoretical [12] and experimental [13] work has demonstrated that CDI depends critically for its success on near-perfect spatial coherence in the illuminating beam. Phase curvature in the incident field can relax this requirement [12] but a small degree of partial spatial coherence may still result in a failure to retrieve the phases of x-ray data. Experiments performed with optical lasers produce data that are reported to converge consistently [14]. In this Letter we develop a method that lifts the restriction to fully coherent illumination in CDI, and demonstrate the effectiveness of the approach by recovering images from partially coherent diffraction data obtained with an undulator source. Our method will open the way to coherent imaging using less coherent sources. Examples of further applications include electron diffraction [15] for atomic resolution of nanoclusters, nanotubes, and potentially, single biomolecules, time-resolved x-ray imaging, as additional flux from existing sources will become usable, the x-ray imaging of hard condensed matter and industrial samples through the use of higher energies for which coherence is generally poorer, and more reliable imaging from sources that produce high, but imperfect, coherence [11].

A formal framework describing diffractive imaging using partially coherent illumination has been presented elsewhere [12]. It was shown that a thin object with complex transmission function, $T(\boldsymbol{r})$, where $\boldsymbol{r}$ denotes position in a plane transverse to the optical axis, illuminated with a partially coherent quasi-monochromatic field defined by a mutual optical intensity (MOI) $J(\boldsymbol{r}_1, \boldsymbol{r}_2)$ produces a far-zone intensity distribution described by

$$I(\boldsymbol{k}) = \int J(\boldsymbol{r}_1, \boldsymbol{r}_2) T(\boldsymbol{r}_1) T^*(\boldsymbol{r}_2) \exp[-i\boldsymbol{k} \cdot (\boldsymbol{r}_1 - \boldsymbol{r}_2)] d\boldsymbol{r}_1 d\boldsymbol{r}_2, \tag{1}$$

where $\boldsymbol{k}$ is the transverse component of the scattered k vector.

The coherent-mode model proposed by Wolf [16] exploits the positive-definite nature of $J(\boldsymbol{r}_1, \boldsymbol{r}_2)$ to write it in the form

$$J(\boldsymbol{r}_1, \boldsymbol{r}_2) = \sum_{n=1}^{N} \mu_n \psi_n(\boldsymbol{r}_1) \psi_n^*(\boldsymbol{r}_2), \quad (2)$$

in which the real, non-negative numbers, μ_n, describe the occupancies of the modes, $\psi_n(\boldsymbol{r})$, which are orthonormal and mutually incoherent. In this formulation, the intensity of the diffraction pattern is described by

$$I(\boldsymbol{k}) = \sum_{n=1}^{N} \mu_n I_n(\boldsymbol{k}), \quad (3)$$

where $I_n(\boldsymbol{k})$ is the intensity of the coherent diffraction pattern produced by propagating the two-dimensional function $T(\boldsymbol{r})\psi_n(\boldsymbol{r})$ to the far zone. This transforms Eq. (1) into a rapidly convergent sum of products of two-dimensional Fourier transformations. The case where $N = 1$ corresponds to full spatial coherence and so the conventional formulation of CDI emerges as a limiting case of this more general theory. This approach is readily extended to imaging techniques that employ electron scattering [15] by replacing $J(\boldsymbol{r}_1, \boldsymbol{r}_2)$ with the first-order electronic density matrix, $\rho(\boldsymbol{r}_1, \boldsymbol{r}_2)$ [17], and the optical modes by the corresponding natural orbital basis [18].

Here, building on work in the frequency domain [19], we show that high quality images can be obtained with partially coherent light by propagating with a field containing a small number of spatial modes. The essence of our multimodal algorithm is as follows: A field with a mutual optical intensity function described by Eq. (2) is used to form an estimate of the partially coherent field leaving the sample. The field is then propagated to the detector plane using Eq. (3) where the measured intensity is imposed on the field, rescaling the amplitudes of the modes and leaving their phases intact. The highest occupancy mode is then propagated from the detector plane to the sample plane where, because the assumption that the source is quasimonochromatic ensures that $T(\boldsymbol{r})$ operates equally on each mode in Eq. (3), the sample plane support constraint is applied. We note that any mode could be used for this backpropagation step and we here choose the highest occupancy mode as it contains by far the most energy and so is the most accurately measured.

Each cycle of the algorithm here involves 50 iterations of the error reduction [20] algorithm followed by 50 iterations of the hybrid input-output [21] algorithm. A further 100 iterations of the error reduction algorithm are performed after which the object support is refined using the shrink-wrap algorithm [22]. This cycle is repeated until convergence is achieved; six repetitions is typical. The algorithm was tested on simulated data for a range of incident coherence conditions and it was found that the transverse coherence length in the Gaussian-distributed illuminating radiation had a permissible uncertainty of around $\pm 10\%$ for values smaller than the object, with a significantly greater uncertainty permissible for longer coherence lengths. Good convergence was achieved in cases in which the coherence length was not less than half the largest transverse dimension of the object.

The complete coherence function has been recovered for the radiation from an undulator source [23]. It was found that the MOI at the experiment is accurately described by the statistically stationary Gaussian form,

$$J(\boldsymbol{r}_1, \boldsymbol{r}_2) = I_0 \exp\left[-\left(\frac{|x_1 - x_2|^2}{\ell_x^2} + \frac{|y_1 - y_2|^2}{\ell_y^2}\right)\right], \quad (4)$$

where Eq. (4) supplies the definition of the horizontal and vertical coherence lengths, ℓ_x and ℓ_y, respectively, used here. The modal structure of $J(\boldsymbol{r}_1, \boldsymbol{r}_2)$ was determined using a procedure published elsewhere [24]. It was found that, for the 2-ID-B beam line at the Advanced Photon Source [25] used in the experiments reported here, only three coherent modes contribute significantly to the expansion of $J(\boldsymbol{r}_1, \boldsymbol{r}_2)$. The Gaussian form of the source distribution in synchrotron sources will result in an MOI of the functional form given in Eq. (4). However, it is to be expected that the presence of optical components in the beam line may influence the precise form to some degree.

The diffraction experiment was conducted using 1.4 keV x rays at beam line 2-ID-B [25]. The coherence length of the incident radiation was varied for this experiment via the monochromator exit slit setting, which defines the effective source size [9]. A set of Young's pinholes were placed 8 m from the exit slit of the monochromator and the fringes were recorded for 1.4 keV x rays using a Princeton Instruments PIXIS CCD detector, which had $2,048 \times 2,048$ pixels, each 13.5 μm square and located 4.4 m from the pinholes. Two horizontal exit slit settings for the monochromator were chosen (5 μm and 525 μm), which span the range from high coherence (5 μm setting) to low coherence (525 μm setting) in the illumination [9] in the horizontal direction. The interference pattern for the lower coherence setting is shown in Fig. 1(a). Here, the two 0.87 μm pinholes are separated by 12.7 μm. The precise dimensions of the Young's pinhole set were determined *post-facto* by a fitting procedure [9]. The data were fitted using an expression of the form in Eq. (4) to determine the coherence lengths which, in the horizontal direction, was determined to be (9.7 ± 0.5) μm. The coherence length in the vertical direction for this system is known to be so large (>1 mm) that full spatial coherence was assumed, modeled by a single spatial mode. The 5 μm exit slit setting resulted in fringes consistent with full coherence.

The CDI experiment used the sample shown in Fig. 1(b). The sample consists of a set of apertures milled by a focused ion beam into a gold substrate of nominal 3 μm thickness which therefore has negligible transmission for the 1.4 keV x rays used here. The sample was placed 11 m from the exit slit of the monochromator and 1.4 m before the CCD detector described above. The detector was aligned so that the diffraction pattern was centered on the detector. Each data frame was corrected for background

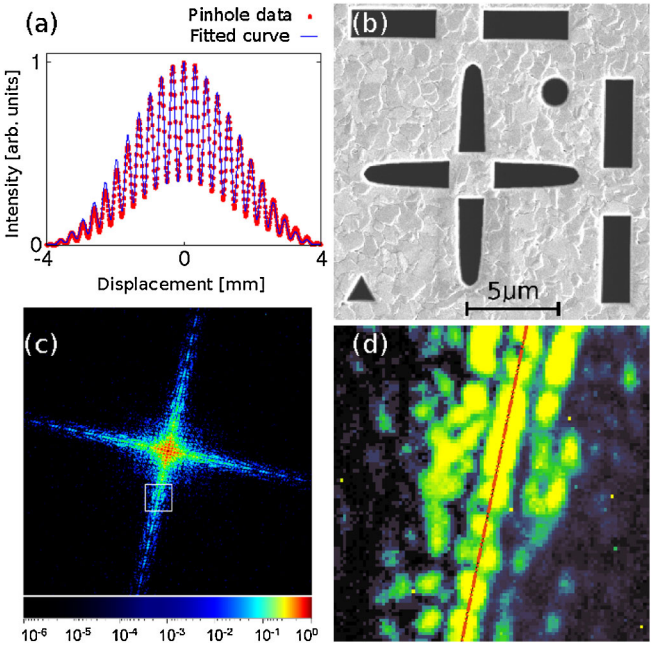

FIG. 1 (color online). (a) Young's interference fringes used to measure the coherence length of the x rays at the plane of sample. The data are analyzed using a Gaussian statistically stationary model for the coherence function. The exit slit of the monochromator had a nominal width of 525 μm for these data. (b) Scanning electron micrograph of the sample used in the CDI experiments. The sample is drilled in gold using a focused ion beam. The sample dimensions are shown. (c) Diffraction data from the sample in (a) obtained using 1.4 keV x rays. This data was obtained using the highest coherence available. The color bar along the bottom of the image indicated the relative intensity of the measured data, with the highest intensity normalized to unity and corresponds to a scattering vector at the detector corners with magnitude 9.8 nm^{-1}. (d) Detail from the data. The panel shows the region of the data contained in the white box seen in (b) for highly coherent data to the left of the red line and low coherence data to the right.

signal and thresholded before 600 consecutively recorded data frames were summed. An example of the diffraction pattern for the highest coherence condition is shown in Fig. 1(c). Detailed images of a section of the diffraction pattern are shown for both high and low coherence in Fig. 1(d). As expected, the visibility of the speckle is reduced in the lower coherence data.

As the sample was further from the exit slit than were the pinholes in the Young's experiment, the coherence length at the sample was assumed to scale linearly on propagation from the double-pinhole plane to the sample plane. We use a factor 11/8 to rescale ℓ_x, corresponding to the ratio of the two distances from the exit slit. Data were reconstructed assuming both full coherence and by using the measured coherence properties and the algorithm described here. The reconstructed sample-plane wave magnitude for the low coherence data obtained using the multimode algorithm above is shown in Fig. 2(a). The reconstruction is remarkably accurate; reconstructions from different random starting guesses did not produce significant differences in the converged solution. By comparison, the assumption of full spatial coherence and the use of a single mode fails to find a satisfactory solution for the phase of the partially coherent diffraction pattern, as seen in Fig. 2(b).

Further data were obtained under conditions approaching full spatial coherence of the illumination. An estimate of the coherent modes was also performed for this data on the assumption that the horizontal coherence length was 40 μm; we expect that the practical impact of an inaccurate coherence length will be small provided the estimate and the correct value are both much larger than the diffracting object. This resulted in a transmission function, displayed in Fig. 2(c). The fully coherent (single-mode) implementation of the algorithm was able to recover the transmission function of the object, Fig. 2(d), though the reconstruction displays artifacts inconsistent with the known uniformity of the illumination. The reconstruction using multimodal propagation is significantly more uniform in intensity over the apertures than is the single-mode result, indicating that the effects of partial spatial coherence can profitably be included in the analysis of synchro-

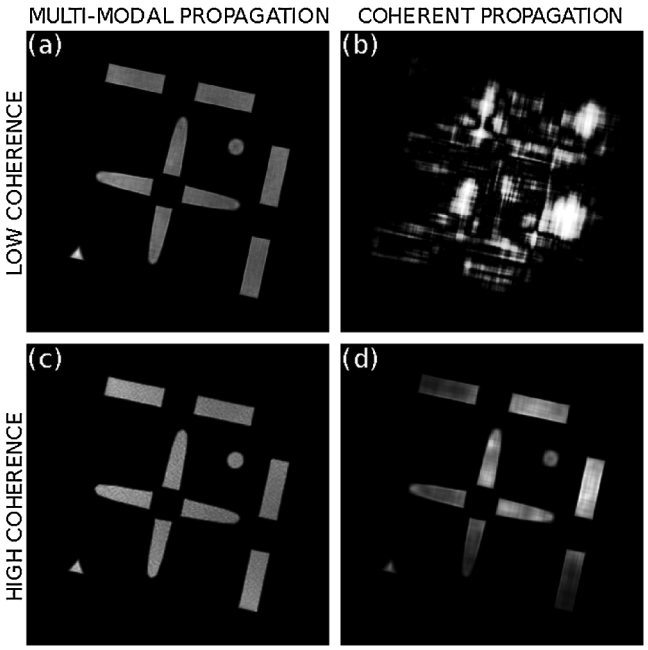

FIG. 2. (a) Reconstruction of the magnitude of the wave leaving the sample using the known coherence information (labeled "multimodal" propagation). (b) A reconstruction of the same data in identical conditions except that full spatial coherence is assumed (labeled "coherent" propagation). We were not able to obtain a reconstruction from this data under this assumption. (c) Reconstruction of the high-spatial coherence (5 μm exit slit setting) data using the algorithm that allows for a deviation from perfect coherence. (d) Reconstruction using an algorithm that assumes perfect spatial coherence.

tron data even when they are obtained with a spatial coherence several times larger than the linear dimension of the object.

The spatial resolution was deduced by examining the aperture boundaries in the transmission function recovered from the low coherence data. An error function was fitted across an aperture edge at a number of points from which we obtained a spatial resolution of (65 ± 10) nm. This is consistent with the resolution of 55 nm predicted by Abbé theory using the maximum diffraction angle at which x rays have been measured. The similarity of Figs. 2(a) and 2(c) demonstrates that the use of partially coherent illumination in diffractive imaging does not significantly degrade the spatial resolution available.

In conclusion, we have shown that partial spatial coherence can be incorporated into the reconstruction of CDI images and that the method enables reconstructions in cases precluded by conventional approaches. The inclusion of partial coherence reduces the artifacts in reconstructions obtained using highly coherent illumination and promises to substantially improve imaging consistency, reliability and quality for all applications of CDI. We anticipate that it can also be extended to higher energy and lower brilliance x-ray sources to compensate for their shorter coherence lengths. An appropriate recasting of the method will further allow its extension to partially coherent electron sources.

L. W. acknowledges the support of a Melbourne Postgraduate Research grant. The authors acknowledge the support of the Australian Research Council through its Centres and Federation programs. The authors thank Dushyant Kumar, Grant Baumgardner, and Ray Conley for fabricating the Young's pinhole set. The use of the Advanced Photon Source is supported by the U.S. Department of Energy, Office of Science, Office of Basic Energy Sciences, under Contract No. DE-AC02-06CH11357.

[1] J. Miao, D. Sayre, and H. N. Chapman, J. Opt. Soc. Am. A **15**, 1662 (1998).
[2] R. H. T. Bates, Optik **61**, 247 (1982).
[3] R. Neutze *et al.*, Nature (London) **406**, 752 (2000).
[4] H. N. Chapman *et al.*, Nature Phys. **2**, 839 (2006).
[5] H. N. Chapman *et al.*, J. Opt. Soc. Am. A **23**, 1179 (2006).
[6] G. J. Williams *et al.*, Phys. Rev. Lett. **97**, 025506 (2006); B. Abbey *et al.*, Nature Phys. **4**, 394 (2008); P. Thibault *et al.*, Science **321**, 379 (2008).
[7] P. Thibault *et al.*, Acta Crystallogr. Sect. A **62**, 248 (2006); G. J. Williams *et al.*, Cytometry Part A **73A**, 949 (2008).
[8] A. Barty *et al.*, Phys. Rev. Lett. **101**, 055501 (2008); M. A. Pfeifer *et al.*, Nature (London) **442**, 63 (2006); B. Abbey *et al.*, Appl. Phys. Lett. **93**, 214101 (2008).
[9] D. Paterson *et al.*, Opt. Commun. **195**, 79 (2001).
[10] F. Pfeiffer *et al.*, Phys. Rev. Lett. **94**, 164801(2005).
[11] A. Singer *et al.*, Phys. Rev. Lett. **101**, 254801 (2008).
[12] G. J. Williams *et al.*, Phys. Rev. B **75**, 104102 (2007).
[13] L. W. Whitehead *et al.*, Phys. Rev. B **77**, 104112 (2008).
[14] J. C. H. Spence, U. Weierstall, and M. Howells, Phil. Trans. R. Soc. A **360**, 875 (2002).
[15] W. J. Huang *et al.*, Nature Phys. **5**, 129 (2009).
[16] E. Wolf, J. Opt. Soc. Am. **72**, 343 (1982).
[17] J. Frank, Optik **38**, 519 (1973).
[18] P. O. Lowdin, Phys. Rev. **97**, 1474 (1955).
[19] B. Chen *et al.*, Phys. Rev. A **79**, 023809 (2009).
[20] R. W. Gerchberg and W. O. Saxton, Optik **35**, 237 (1972).
[21] J. R. Fienup, Appl. Opt. **21**, 2758 (1982).
[22] S. Marchesini *et al.*, Phys. Rev. B **68**, 140101(R) (2003).
[23] C. Q. Tran *et al.*, Opt. Lett. **30**, 204 (2005); C. Q. Tran *et al.*, Phys. Rev. Lett. **98**, 224801 (2007).
[24] S. Flewett *et al.*, Opt. Lett. **34**, 2198 (2009).
[25] I. McNulty *et al.*, Rev. Sci. Instrum. **67**, 3372 (1996).